Environmental stability of actively mode locked fibre lasers

Environmental Stability of Actively Mode-Locked Fibre Lasers

Calum H. Hill[a,b], Stephen T. Lee[a], Derryck T. Reid[b], Ghaya Baili[c] and John Davies[d]
[a]Thales OME, 1 Linthouse Road, Glasgow, UK, G51 4BZ;
[b]Ultrafast Optics Group, School of Engineering and Physical Sciences, Heriot-Watt University, Edinburgh, UK, EH14 4AS;
[c]Thales Research and Technology, 1 Avenue Augustin Fresnel, 91120, Palaiseau, France;
[d]Thales DMS, Manor Royal, Crawley, UK, RH10 9AD

ABSTRACT

Lasers developed for defence related applications typically encounter issues with reliability and meeting desired specification when taken from the lab to the product line. In particular the harsh environmental conditions a laser has to endure can lead to difficulties. This paper examines a specific class of laser, namely actively mode-locked fibre lasers (AMLFLs), and discusses the impact of environmental perturbations. Theoretical and experimental results have assisted in developing techniques to improve the stability of a mode-locked pulse train for continuous operation. Many of the lessons learned in this research are applicable to a much broader category of lasers.

The AMLFL consists of a fibre ring cavity containing a semiconductor optical amplifier (SOA), an isolator, an output coupler, a circulator, a bandpass filter and a modulator. The laser produces a train of 6-ps pulses at 800 nm with a repetition rate in the GHz regime and a low-noise profile. This performance is realisable in a laboratory environment. However, even small changes in temperature on the order of 0.1 ^{o}C can cause a collapse of mode-locked dynamics such that the required stability cannot be achieved without suitable feedback. Investigations into the root causes of this failure were performed by changing the temperature of components that constitute the laser resonator and observing their properties.

Several different feedback mechanisms have been investigated to improve laser stability in an environment with dynamic temperature changes. Active cavity length control will be discussed along with DC bias control of the Mach-Zehnder modulator (MZM).

Keywords: Fibre Laser, Active Mode-locking, Temperature, Environmental Stability, Stabilisation

1. INTRODUCTION

Mode-locked fibre lasers are a well-developed technology with inherent reliability advantages when compared to solid state laser designs[1-3]. While there has been much research on mode-locked lasers in a lab setting there is currently a lack of published work that details how actively mode-locked lasers perform under environmental duress. The work that has been performed is limited in scope, confining its analysis to specific applications or focusing on the overall system[3-8] . To understand how to design robust fibre lasers it is necessary to quantify environmental behaviour at a component level and its impact on system level performance. This information is critical when designing lasers for industrial and defence applications where 24/7 operation is expected across a broad range of environmental conditions. Typically, any hardware designed for the field will have a requirement to operate within a specified temperature range. There will also be requirements for shock, vibration, humidity, salinity and radiation exposure. These need to be considered in the design stage of any laser system.

There has been an increasing interest in using semiconductor optical amplifiers (SOAs) as the gain medium in mode-locked lasers due to their fast gain dynamics, high efficiency, small size and ease-of-use. Some work has been done in generating high-frequency, low-noise pulse trains using SOAs as the gain medium in a fibre architecture[1,9,10]. SOAs are preferable in this regard to fibre amplifiers as the long fluorescence lifetimes associated with doped fibres can lead to relaxation oscillations that limit noise performance[11]. In addition the short carrier lifetimes of semiconductor amplifiers favour high repetition rates[12].

Various architectures have been employed to reduce the noise within the laser, often using a free space element within the cavity such as an etalon or allowing optical frequency to drift[11, 13-16]. Often active feedback has been employed to

improve laser stability, however published work only details how to do this for small changes in ambient conditions[13,15]. Lasers with an all-fibre architecture are alignment-free, vibration insensitive and naturally resistant to humidity and salinity levels. These properties come directly from the silica fibre used to construct components. It is a natural progression then to leverage these advantages to environmentally robust mode-locked lasers, however temperature changes are still expected to cause problems in a number of areas. The work here focuses on semiconductor based actively mode-locked fibre lasers and how they respond to changes in temperature.

2. LASER DESIGN

The laser to be discussed is presented in Fig. 1. The gain medium was an SOA with a central wavelength of 800 nm with a maximum output power of 20 mW. It operates with an external, all-fibre cavity. The cavity contained a circulator, isolator, output coupler, Mach-Zehnder modulator (MZM) and a chirped Bragg grating. All components and fibre were polarisation maintaining. The laser was 15.3 m long which resulted in a fundamental cavity frequency of 13.4 MHz. The laser was intended to operate around 6 GHz so harmonic mode-locking was necessary. Thus the MZM applies a loss modulation at an integer multiple of the fundamental frequency, in this case the 448th to give a repetition rate of 6.003 GHz. When mode-locked the laser typically produced between 1 mW and 5 mW of average power.

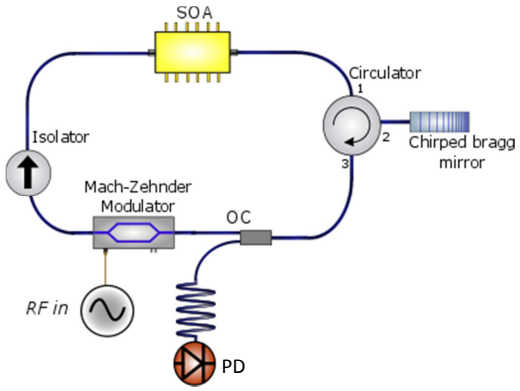

Figure1. Schematic representation of actively mode-locked fibre laser. OC: Output coupler. PD: Fast photodiode.

Unlike fundamental mode-locking, a harmonically mode-locked laser will have many pulses oscillating in the cavity at the same time[17]. The MZM acted as the mode-locking mechanism by providing a periodic loss modulation to the laser cavity and was driven by a frequency synthesiser. The chirped Bragg grating had a 1nm bandwidth and had a large positive dispersion parameter to give the cavity an overall anomalous dispersion. It has been shown experimentally that pulse stability is improved in the anomalous dispersion regime for this laser and that a larger dispersion value for the grating is better. There are two primary reasons why this is the case and both centre around having dispersion stretched pulses incident on the laser components.

Firstly the MZM can introduce amplitude and phase noise if the peak of the pulse is not perfectly aligned with the peak transmission window of the MZM. Having longer pulses incident on the MZM allows this mismatch to be minimised. The second effect is much more pronounced. The gain medium within the SOA is highly nonlinear and experiences strong self-phase modulation that limits pulse stability and the minimum achievable pulse widths[18]. The impact of this SPM effect can be minimised by having longer pulses propagate in the cavity.

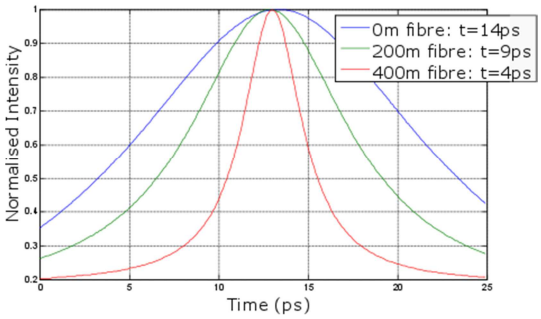

Figure 2. Autocorrelation traces of laser pulse normalised to unity amplitude. Blue: Laser output with no compression. Green: Laser output after 200 m of fibre. Red: Laser output after 400 m of fibre.

The pulses were highly chirped when they were coupled out of the laser cavity as the Bragg grating gave the cavity a net anomalous dispersion. However, the fibre used had a strong normal dispersion and propagation through a long length of fibre was used to compress the pulse down to a few ps. This can be seen in Fig. 2.

3. LASER CHARACTERISATION

It is imperative that the synthesizer drive frequency precisely matches an integer multiple of the cavity mode spacing for stable mode-locking to occur. The difference between a well matched drive frequency and one that is slightly detuned can be seen Fig. 3**.** Figure 3a and 3b show a drive frequency that was well matched to the resonant cavity harmonic. Here the noise in the modes surrounding the drive frequency have been suppressed. Figure 3c and 3d shows the effect a small detuning of cavity resonance and drive frequency had, the detuning is720 kHz. Here the noise floor has increased and more noise is present in the satellite modes. The linewidth of the carrier has also broadened. This has negative consequences for the stability of the pulse train. We will see in Section 5 that far greater frequency mismatches were caused by changes in environmental conditions.

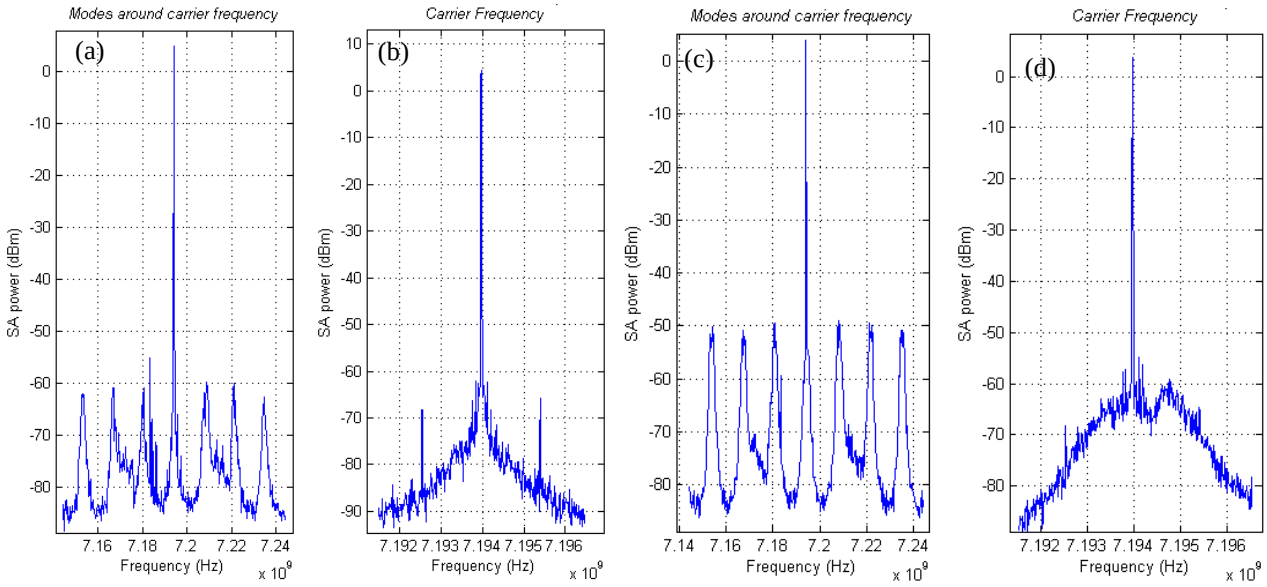

Figure 3. Measured RF spectra of photodiode signal. Laser has a pulse repetition rate of 7.2 GHz. (a&b) RF spectrum of optimised pulse train centred at carrier frequency. (a) 100 MHz Span, (b) 10 MHz span. (c&d) RF spectrum of pulse train with detuned cavity frequency. (c) 100 MHz span, (d) 10 MHz span.

The laser design used in this paper was intentionally simple and did not contain any feedback mechanisms to improve the noise performance. This was to allow simpler diagnoses of root causes of temperature dependent behaviour. With that in mind it is worth taking a moment to consider what variables might affect pulse stability when subjected to a change in temperature. Silica glass has a low coefficient of thermal expansion[5]; however its thermo-optic coefficient is far more significant. While the physical length of fibre did not change by much, the optical path length varied significantly over the temperature range of interest (0 ^{o}C to 50 ^{o}C). The change in optical length (ΔL_o) can be calculated using.

$$\Delta L_o = (\alpha + \beta) n \Delta T L \quad (1)$$

Where $\alpha = 0.55 \times 10^{-6}$ ^{o}C^{-1} is the coefficient of thermal expansion for fused silica, $\beta = 11.5 \times 10^{-6}$ ^{o}C^{-1} is the thermo-optic coefficient for fused silica[5], n is the refractive index, $\Delta T = 50$ ^{o}C is the temperature change and L=15.3 m is the length of fibre in the cavity. Using these values an optical path length increase of 13.4 mm was expected. Various stabilisation methods actively change the length of the laser cavity to reduce modes, but these do not consider the much longer path length changes that will need to be considered here[13, 16, 19].

It is known that the bias voltage used to control the MZM can drift under normal operating conditions and complex behaviour has been observed[20] when changing the ambient temperature. The ability of the laser to obtain stable mode-locking with a low noise pulse train is critically dependent on this voltage so active feedback will be required for long term stable operation.

4. TEMPERATURE DEPENDENCE OF COMPONENTS

Figure 4a shows a generic schematic of the experimental setup used to investigate the temperature behaviour of the individual components that make up the laser. The SOA acted as an ASE source and the chirped grating was present to give the incident light a more experimentally relevant optical bandwidth. Experiments were performed from 0 ^{o}C to 50 ^{o}C with 10 ^{o}C increments between measurement points. The first item to be investigated was the loss behaviour of the fibres and the connectors. The fibre used was HP780 polarisation maintaining fibre. The attenuation in fibre did not change significantly over the temperature range investigated here. Temperature dependent loss from a single connector can be seen in Fig. 1b. The loss from a single connector increased by 0.1 dB from 0^{o} C and peaking at 30^{o}C. Care was taken to keep fibre ferrule heads clean, but large values for loss were recorded nonetheless. This is attributed to imperfect alignment of stress rods in the fibre. Loss variation is important as it changes the power in the laser, this can couple directly to pulse stability. If the intracavity power decreases, the SOA may no longer be completely saturated leading to a higher proportion of ASE in the cavity.

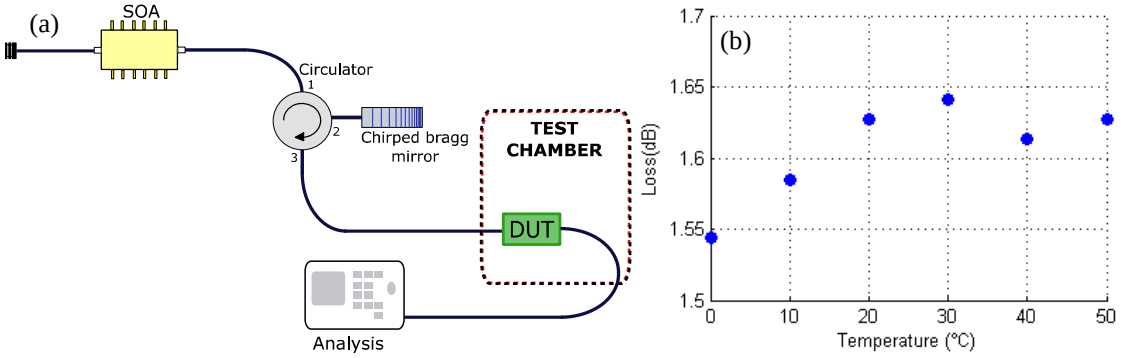

Figure 4: (a) Experimental set up used for investigating temperature dependence of various fibre components. (b) Loss as a function of temperature for tight key PM connectors.

4.1 Isolator and Circulator

The forward performance of the isolator was tested for temperature dependence and its loss behaviour can be seen in Fig. 5a. Here a minimum loss of 1.4 dB is observed at 30 ^{o}C which rises to 2.7 dB at 0 ^{o}C. This intracavity loss variation is a major indicator of potential temperature instabilities within the oscillator. Its origin can be explained by considering the operation of a polarisation sensitive Faraday isolator[21, 22] and what changes with temperature. The Verdet constant is

temperature dependent and describes the strength of the Faraday Effect in a particular material; in addition the field strength of a permanent magnet has a strong temperature dependence. With these two effects in combination the degree of polarisation rotation in the Faraday isolator, and thus the loss, are varying with temperature.

Figure 5b shows the loss induced by a single pass of the circulator as a function of temperature. The circulator also uses the Faraday Effect to control the direction of light, so the same argument presented above applies. Thus it is no surprise that the isolator and circulator display the same loss profile, especially as they are from the same manufacturer. The loss variation from the circulator is much smaller so it becomes less of a priority to eliminate this loss source than the isolator.

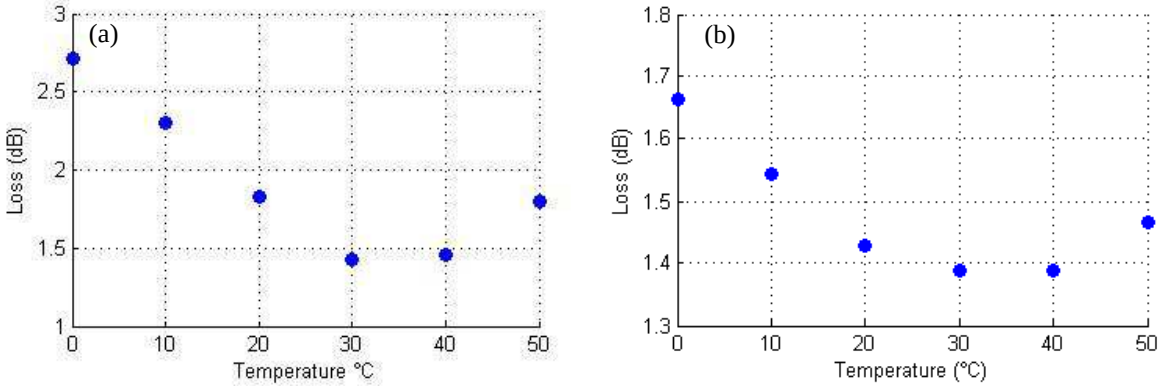

Figure 5. (a) Isolator loss as a function of temperature. (b) Circulator loss as a function of temperature.

4.2 Chirped Fibre Bragg Grating

A chirped FBG reflects different wavelengths at different positions along the fibre. To do this the periodicity of the grating increases or decreases along its length. As temperature increases we would expect a global increase in refractive index and overall length of the grating. This will change the $\lambda/4$ condition for high reflectivity and move the centre wavelength of reflection to higher wavelengths. Experimentally this can be seen in Fig. 6b where the central wavelength of the FBG behaved as expected. However, the wavelength drift was < 1 % of the gain bandwidth of the SOA and did not have an influence on stable laser operation. The output power of the FBG decreases with temperature as seen in Fig. 6a, but again the difference is small enough that it is unlikely to affect the gain dynamics of the laser.

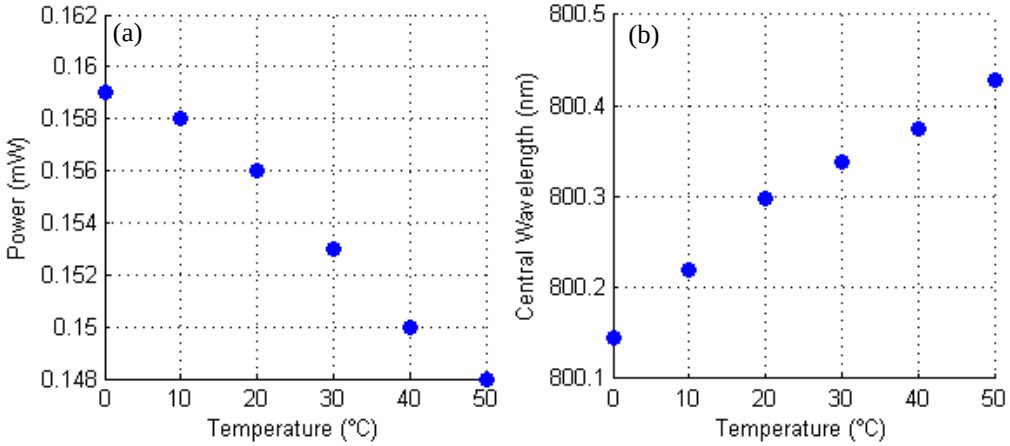

Figure 6. (a) Power reflected by FBG as a function of temperature. (b) Central wavelength of reflection of FBG as measured by an optical spectrum analyser.

4.3 Mach-Zehnder Modulator

The final component that was investigated in this manner was the MZM. The transmission through the MZM is sinusoidally dependent on the DC bias voltage applied to it, when there is no RF signal incident. It was instructive in this case to see how transmission through the MZM responded to a change in temperature. The results in Fig. 7a applied a 10 ^{o}C temperature change in 15 minutes while the output power level was continuously monitored. It is clear that the effective bias voltage on the MZM changed through 1.7 cycles of the MZM transfer function. For this device that equates to a voltage build-up of 7.8 V (V_{π}=2.3 V) which then took > 10 hours to stabilise again. We can see a less dramatic, but still significant, change in transmission arising from a 1 ^{o}C change over 20 minutes in Fig. 7b. This, much more realistic, temperature change still caused a change in power transmitted from 43 µW to 19 µW which corresponds to a voltage build-up of 0.6 V.

Fundamentally, this transmission change is caused by a charge imbalance between the two arms of the MZM which causes the relative voltage between them to change. The cause of this arises from a complex interplay between pyroelectric, photorefractive and photoconductive phenomenon in electro-optic materials[20, 23]. In order for a laser containing a MZM to function as required it is necessary to have some active feedback to stabilise the wild temperature response of the MZM.

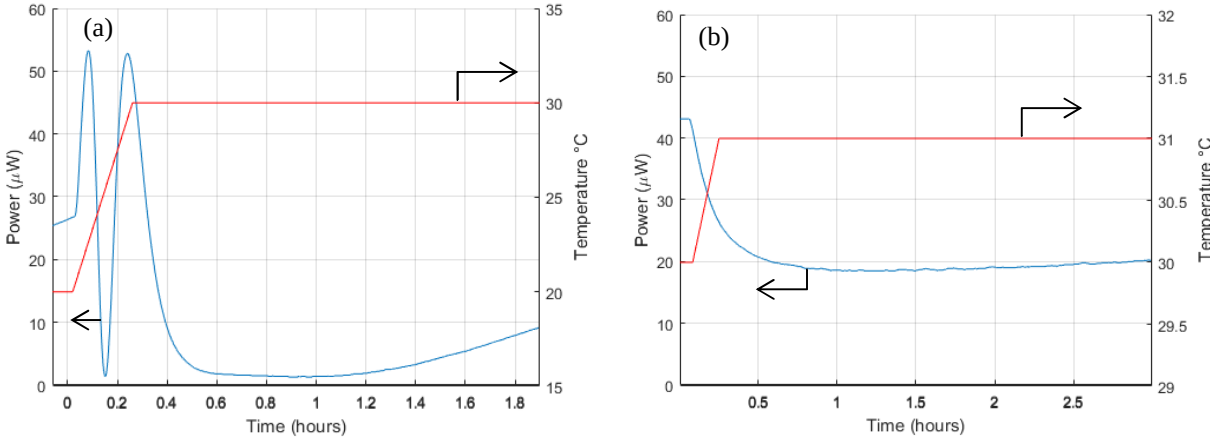

Figure 7. (a) Transmission response of a MZM when subject to a 10 ^{o}C change in ambient temperature with no stabilisation. (b) The transmission response of a MZM when subject to a 1 ^{o}C change in ambient temperature.

5. TEMPERATURE DEPENDENCE OF LASER PARAMETERS

5.1 Laser Stability

Experiments were performed with the entire laser contained within the environmental chamber, although the photodiode, drive electronics and diagnostic equipment remained external. It was interesting to note how the mode structure changed with temperature as this give a direct indicator of pulse train stability. The bias point of the MZM needed to be carefully set for each measurement as even small drifts caused a collapse of mode-locked laser dynamics. This made optimisation difficult and not entirely repeatable without an automated method of setting the bias point of the MZM.

5.2 Cavity Length

The shift in cavity fundamental frequency corresponds to a change in optical path length in the cavity. An attempt was made to measure this directly by looking for the position of the peaks in adjacent cavity modes. However the features on adjacent modes were rarely identical, particularly when resolution on the spectrum analyser was decreased and further fine structure was revealed. To circumvent this, the drive frequency was matched precisely to the 448th cavity mode for each temperature as the matching point was easily observable on the RF spectrum analyser. This is then easily converted into a cavity length, the results are shown in Fig. 8**.** Where each measurement point was taken with the laser fully optimised.

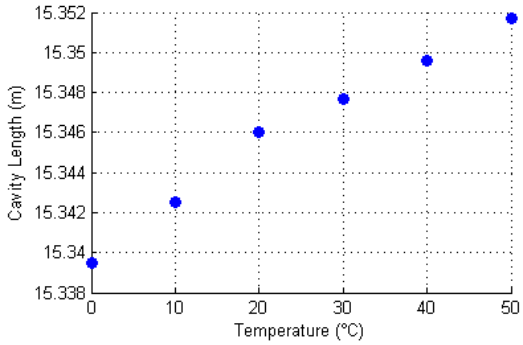

Figure 8. Cavity length of the laser measured at different temperatures.

What is striking from Fig. 8 is that the effective physical length of the cavity changes by 10.7mm, more appropriately the optical path length changes by 15.6mm. This is a substantial increase from the calculated value of 13.4mm and there are a few probable reasons for this. It is known that the electro-optic material in the MZM has a large thermo-optic coefficient. However given the small size of the MZM device it is unlikely that this contributes a large proportion of the discrepancy. More likely is that expansion and refractive index changes in the isolator and circulator are the dominant sources of error, but the exact cause is unknown.

The effect of this frequency mismatch when not accounted for was catastrophic and quickly lead to a collapse of mode-locked behaviour. Consequences of such a mismatch can be seen directly in the RF spectra in Fig. 9. The laser was optimised at 50^{o}C (Fig. a) and as the temperature is decreased the detuning between drive frequency and cavity mode becomes more significant. At 40^{o}C (Fig. b) the laser is still producing pulses, however additional noise has been introduced to the system and multiple pulse instabilities occur. At 30^{o}C (Fig. c) the output is largely noise with a strong sinusoidal component being introduced by the MZM. Each subsequent reduction in temperature decreased the signal to noise ratio of the carrier frequency.

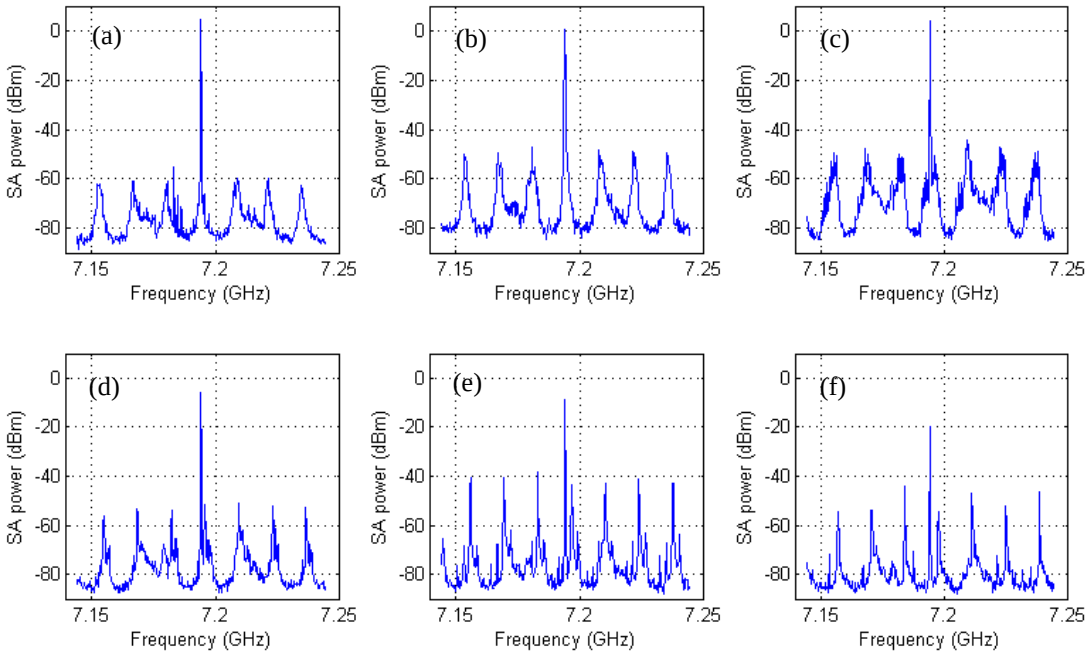

Figure 9. RF spectra of the driving signal and surrounding cavity modes taken at different temperatures. (a) Laser is optimised at 50°C for low noise floor and supermode suppression. (b) 40°C cavity length change has caused detuning of carrier and cavity modes, introducing noise to the system. (c) 30°C frequency mismatch has increased introducing more noise into the surrounding modes. (d) 20°C Visible offset from frequency peaks has caused a dramatic loss of carrier power. (e) 10°C Modes have completely walked off from the carrier. (f) 0°C Carrier and cavity mode are clearly distinct and the reduction that has on carrier Power is evident.

5.3 Output Power

Figure 10 shows the temperature dependence of laser output power. Judging by the distribution of points it is reasonable to conclude that temperature dependent loss in the isolator and circulator is the dominant mechanism responsible for this behaviour. It is also instructive to note that for each measurement the laser was mode-locked and re-optimised for minimum jitter. This leads to a lack of repeatability for power measurements as the optimum bias point is difficult to obtain every time manually. Especially at low and high temperatures when the stability region is smaller. This is compounded by the complicated loss behaviour of the MZM which depends on temperature gradients and is not represented here. By summing the loss contributions profile of loss against temperature can be obtained, as in Fig 10b.

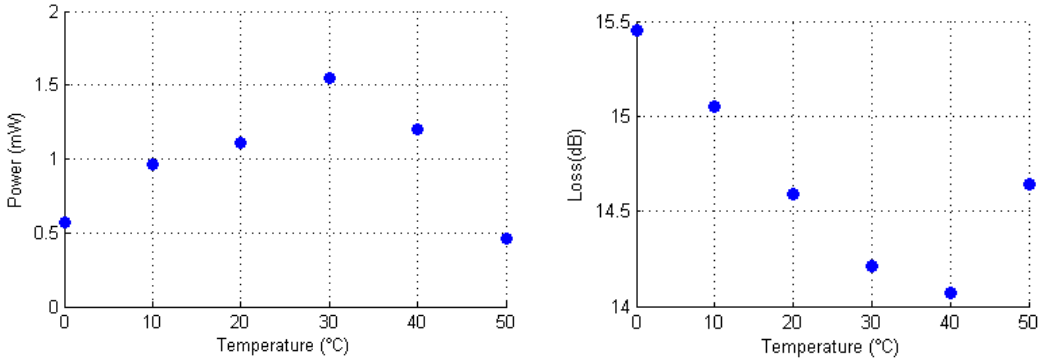

Figure 10. (a) Laser output power as a function of temperature. (b) Summation of laser component losses against temperature.

6. COMPENSATING FOR TEMPERATURE CHANGES

6.1 Cavity Length

In order for the laser to operate over a broad temperature range the cavity length needs to be stabilised. There are a number of techniques that can be used to do this. A promising method for small length changes allows the central wavelength to drift passively to self-stabilise the match between cavity modes and drive frequency[15]. More practically it is possible to change the physical length of the cavity. The easiest way to do this uses a free space translation stage to control the distance between two fibre collimators. However, this removes the advantages of having an alignment free all-fibre cavity. A fibered configuration can only be obtained by stretching the fibre itself to control the cavity length. It is common practice to use piezoelectric transducers to alter the length of fibre by small amounts[13], however this application requires a stretch of >12mm using the limited amount of fibre between components. The small travel afforded by piezoelectric transducers is not appropriate for this application.

In order to do keep the repetition rate constant, fibre was wrapped around cylindrical mandrills which had the distance between them controlled by a translation stage[19]. With 1.5m of fibre wrapped around the mandrills an experiment was performed to see if stretching in this manner would compensate for the temperature induced drifts that have been observed. With the majority of the laser within the chamber, excluding the fibre stretcher, the expected optical path length change is 11.6mm. A physical length change of 8mm will be needed to compensate for this. The laser was optimised at 50^{o}C with the fibre surrounding the mandrills slack. The temperature was reduced in 10^{o}C increments and stretching was performed to match the cavity modes with the driving frequency. The results in Fig. 11 show how much the fibre needed to be stretched at each temperature to achieve low noise mode-locking, this distance was measured using the micrometer that was used to stretch the fibre.

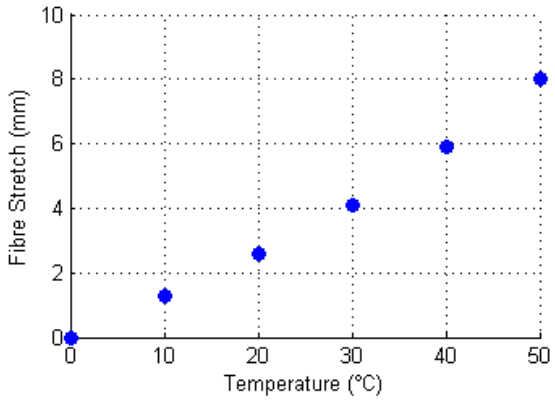

Figure 11. The physical length fibre was stretched in order to tune the cavity length to drive frequency for each temperature.

6.2 Mach-Zehnder Modulator

The laser is extremely sensitive to the bias voltage applied to the MZM. More correctly it requires that a predefined point on the MZM's transfer function be maintained. In a simple transmission experiment this would equate to maintaining a constant optical power. However, once within a laser, the output power cannot be used as a suitable feedback parameter as it is affected by other external factors. There are a number of known techniques for selecting the minimum, maximum or quadrature point of the MZM[24]. However, here it is necessary to be able to reliable operate on an arbitrary point of the sinusoidal transfer curve. In the telecommunications industry this is performed by using pilot tone locking[25]. This involves adding a low amplitude modulation to the modulator at frequency ω. Depending on the MZM's current position on its transfer curve components at ω and 2ω will be produced in different quantities. The ratio between the two spectral densities can be used as a feedback parameter to a PID loop to control the bias voltage and ensure long-lasting laser stability.

Commercial solutions to this problem do exist, but they are expensive and offer reduced flexibility compared to a custom design. A microcontroller was used as the sole component in this stabilisation scheme, specifically the Arduino Due was used as it has access to ARM-math functions and dedicated 12bit DACs, this allows it to quickly perform FFT's and respond with a bandwidth of 20Hz. This is more than sufficient to compensate for thermal effects. The microcontroller

gathers a sample of the signal and performs an FFT to compute the amplitude of the signals at ω and 2ω. An internal PID then acts to maintain the operating point of the MZM to a fixed position.

The effects of this can be seen in Fig. 12, where Fig. 12a is similar to Fig. 7b as it shows how transmission through the MZM changes with no compensation. These can be compared to Fig. 12b where pilot tone locking has taken place. Provided that the amplitude of the pilot tone is sufficiently small compared to the primary RF driving signal then this technique can be used to ensure the laser stays mode-locked against environmental perturbations.

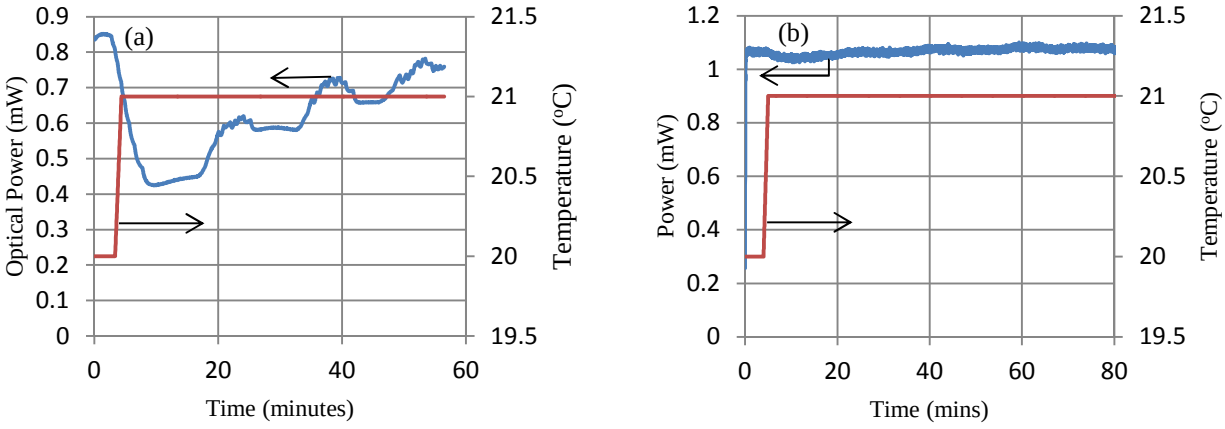

Figure 12. (a) Transmission through MZM when subject to a 1°C temperature increase at t=4minutes with no feedback. (b) Transmission through MZM when subject to a 1°C temperature increase at t=4minutes with pilot tone locking.

7. CONCLUSION AND FUTURE WORK

This work has examined some common parts that make up a fibre laser and investigated how they perform over temperature. While the properties of fibre itself do not change substantially care must be taken in selecting other components. Faraday optical isolators showed strong temperature dependence and due to their bulk can be difficult to thermally stabilise. Improved laser designs would do well to avoid the use of isolators in the cavity if possible. Circulators have a similar problem although it was found to be not as severe. The combined impact of these additional losses at high and low laser temperatures lead to a reduced parameter set for stable mode-locking and variable laser output power.

The Mach-Zehnder modulator was found to be extremely sensitive to temperature with even a 1°C increase causing dramatic transmission changes. Voltage differences that build up between the two arms are disastrous for laser stability and a technique is required to offset this. Pilot tone locking was presented as a possible approach to solving this problem and was implemented using a microcontroller based feedback loop. There are many improvements that can be implemented to improve the performance of this method. Electronics will be developed to better condition the incoming signal for the microcontroller such that FFT results are more accurate. This includes having a more accurate reference voltage for measuring inputs. It is also possible that this method could be performed using all analogue means[25] provided filters with a sufficiently sharp band-edge can be sourced. This would eliminate the need to calculate FFTs and substantially increase the bandwidth of the feedback loop, especially if the microcontroller could be removed from the setup entirely.

Demonstration of stretching the fibre in the laser cavity was performed to illustrate how a constant pulse repetition rate can be obtained over a wide temperature range. Automating this step with a piezoelectric actuator is the logical next step. Both open-loop and closed-loop methods will be investigated.

REFERENCES

[1] Schell, M., Tsuchiya, M.., Kamiya, T., “Chirp and Stability of Mode-Locked Semiconductor Lasers,” IEEE J. Quantum Electron. **32**(I), 1180–1190 (1996).

[2] Fermann, M. E.., Hartl, I., “Ultrafast Fiber Laser Technology,” IEEE J. Sel. Top. Quantum Electron. **15**(1), 191–206 (2009).

[3] Liu, X., Lægsgaard, J.., Turchinovich, D., “Monolithic Highly Stable Yb-Doped Femtosecond Fiber Lasers for Applications in Practical Biophotonics,” IEEE J. Quantum Electron. **18**(4), 1439–1450 (2012).
[4] Wright, M. W., Hemmati, H., “Pulsed fiber amplifiers in simulated space environmental tests,” Proc. SPIE **8971**, 89710B (2014).
[5] Wang, W., Yu, Y., Geng, Y., Li, X., “Measurements of thermo-optic coefficient of standard single mode fiber in large temperature range,” Proc. SPIE **9620**, 96200Y (2015).
[6] Ito, M.., Kimura, T., “Temperature stabilization in semiconductor laser diodes,” IEEE J. Quantum Electron. **17**(5), 796–798 (1981).
[7] Vergnole, S., Kotani, T., Perrin, G., Delage, L.., Reynaud, F., “Calibration of silica fibers for the Optical Hawaiian Array for Nanoradian Astronomy (‘OHANA): Temperature dependence of differential chromatic dispersion,” Opt. Comm. **251**(1), 115–123 (2005).
[8] Brown, D. C.., Hoffman, H. J., “Thermal, stress, and thermo-optic effects in high average power double-clad silica fiber lasers,” IEEE J. Quantum Electron. **37**(2), 207–217 (2001).
[9] Depriest, C. M., Yilmaz, T.., Delfyett, P. J., “Ultralow noise and supermode suppression in an actively mode-locked external-cavity semiconductor diode ring laser,” Opt. Lett. **27**(9), 719–721 (2002).
[10] Roth, J. M., Member, S., Dreyer, K., Collings, B. C.., Knox, W. H., “Fiber Laser Using a Monolithic Semiconductor Optical Amplifier / Electroabsorption Modulator,” IEEE Phot. Tech. Lett **14**(7), 917–919 (2002).
[11] Clark, T. R., Carruthers, T. F., Matthews, P. J.., Duling, I. N., “Phase noise measurements of ultrastable 10 GHz harmonically modelocked fibre laser,” Electron. Lett. **35**(9), 720 (1999).
[12] Storkfelt, N., Mikkelsen, B., Olesen, D. S., Yamaguchi, M.., Stubkjaer, K. E., “Measurement of carrier lifetime and linewidth enhancement factor for 1.5- mu m ridge-waveguide laser amplifier,” IEEE Photonics Technol. Lett. **3**(7), 632–634 (1991).
[13] Rieger, S., Hellwig, T., Walbaum, T.., Fallnich, C., “Optical repetition rate stabilization of a mode-locked all-fiber laser,” Opt. Soc. Am. **24**(4), 4489–4895 (2012).
[14] Davila-Rodriguez, J., Bagnell, K.., Delfyett, P. J., “Frequency stability of a 10 GHz optical frequency comb from a semiconductor-based mode-locked laser with an intracavity 10,000 finesse etalon.,” Opt. Lett. **38**(18), 3665–3668 (2013).
[15] Gee, S., Ozharar, S., Quinlan, F., Plant, J. J., Juodawlkis, P. W., Member, S.., Delfyett, P. J., “Self-Stabilization of an Actively Mode-Locked for Ultralow Jitter,” IEEE Phot. Tech. Lett **19**(7), 498–500 (2007).
[16] Helkey, R., Mar, A., Zou, W., Young, D. B.., Bowers, J., “Mode-locked repetition rate feedback stabilization of semiconductor diode lasers,” Proc. SPIE 1861, 62–71 (1993).
[17] Li, W., Yin, Z., Qiu, J., Wu, J.., Lin, J., “Tunable Active Harmonic Mode-Locking Yb-Doped Fiber Laser With All-Normal Dispersion,” IEEE Photonics Technol. Lett. **25**(23), 2247–2250 (2013).
[18] Agrawal, G. P.., Olsson, N. A., “Self-Phase Modulation and Spectral Broadening of Optical Pulses in Semiconductor Laser Amplifiers,” IEEE J. Quantum Electron. **25**(11), 2297–2307 (1989).
[19] Mei, H., Li, B., Huang, H.., Rao, R., “Piezoelectric optical fiber stretcher for application in an atmospheric optical turbulence sensor,” Appl. Opt. **46**(20), 4371, Optical Society of America (2007).
[20] Ponomarev, R. S., Volyntsev, A. B., Azanova, I. S.., Voblikov, E. D., “Pyroelectric effect in X-cut LiNbO3 optical modulators,” 2013 Int. Conf. Adv. Optoelectron. Lasers (CAOL 2013), 371–372, IEEE (2013).
[21] Kobayashi, K.., Seki, M., “Microoptic grating multiplexers and optical isolators for fiber-optic communications,” IEEE J. Quantum Electron. **16**(1), 11–22 (1980).
[22] Matsumoto, S.., Suzuki, S., “Temperature-stable Faraday rotator material and its use in high-performance optical isolators,” Appl. Opt. **25**(12), 1940 (1986).
[23] Kostritskii, S. M., “Photorefractive effect in LiNbO3-based integrated-optical circuits at wavelengths of third telecom window,” Appl. Phys. B **95**(3), 421–428(2009).
[24] Cho, P. S., Khurgin, J. B.., Shpantzer, I., “Closed-Loop Bias Control of Optical Quadrature Modulator,” IEEE Photonics Technol. Lett. 18(21), 2209–2211 (2006).
[25] Wang, L. L.., Kowalcyzk, T., “A Versatile Bias Control Technique for Any-Point Locking in Lithium Niobate Mach–Zehnder Modulators,” J. Light. Technol. **28**(11), 1703–1706 (2010).